Phase diagram and calorimetric properties of $NaFe_{1-x}Co_xAs$

A. F. Wang, X. G. Luo, Y. J. Yan, J. J. Ying, Z. J. Xiang, G. J. Ye, P. Cheng, Z. Y. Li, W. J. Hu, and X. H. Chen*

Hefei National Laboratory for Physical Science at Microscale and Department of Physics, University of Science and Technology of China, Hefei, Anhui 230026, People's Republic of China

(Received 21 April 2012; revised manuscript received 21 May 2012; published 18 June 2012)

We measured the resistivity and magnetic susceptibility to map out the phase diagram of single crystalline $NaFe_{1-x}Co_xAs$. Replacement of Fe by Co suppresses both the structural and magnetic transitions; however, it also enhances the superconducting transition temperature (T_c) and superconducting component fraction. Magnetic susceptibility exhibits temperature-linear dependence in high temperatures up to 500 K for all the superconducting samples, but such behavior suddenly breaks down for the nonsuperconducting overdoped crystal, suggesting that the superconductivity is closely related to the T-linear dependence of susceptibility. Analysis on the superconducting-state specific heat of the optimally doped crystal provides strong evidence for a two-band s-wave order parameter with gap amplitudes of $\Delta_1(0)/k_BT_c = 1.78$ and $\Delta_2(0)/k_BT_c = 3.11$, being consistent with the nodeless gap symmetry revealed by angle-resolved photoemission spectroscopy experiment.

DOI: 10.1103/PhysRevB.85.224521 PACS number(s): 74.70.Xa, 74.25.Dw, 74.25.Bt, 74.20.Rp

I. INTRODUCTION

Superconductivity in the iron-based superconductors, just like that in cuprates, emerges in the proximity to magnetically ordered state, so the magnetic interactions are considered to play a key role in the mechanism of such high-T_c superconductivity. Accordingly, a central issue for the iron-based superconductors is whether a spin density wave (SDW) follows a local moment or a Fermi surface nesting picture because this is correlated to the nature of the pairing force responsible for the superconductivity.[1–4] The interplay between magnetism and superconductivity has been extensively investigated in the doped $AeFe_2As_2$ (the so-called 122 system, Ae = alkali earth, alkali, and Eu) family due to the easiness of obtaining sizable and high-quality single crystals.[5] The phase diagram, through the measurements of electrical transport, magnetism (susceptibility, μSR, neutron scattering, NMR and so on), crystal structure, and so on, has been well studied in such 122 single crystals.[6–12] However, for the doped NaFeAs system (the so-called 111 system), studies for phase diagram were performed only on polycrystalline samples[13,14] but not on single crystalline ones due to the hardness to grow high-quality single crystals and the difficulty of controlling the doping concentration. For the same reason, little work has been done to elucidate the symmetry of the superconducting gap of the doped NaFeAs system,[15–17] although quite a few studies have been carried out to explore the superconducting gap structure in the isostructural LiFeAs by either specific heat or heat transport or angle-resolved photoemission spectroscopy (ARPES).[18–22] Even for these few studies on the symmetry of the supercondcuting gap of the doped NaFeAs, the results are inconsistent with each other. ARPES, scanning tunneling microscopy (STM), and the heat transport experiments revealed nodeless gaps;[16,17,23] however, the measurements of the penetration depth suggested gaps with nodes.[15]

NaFeAs is established in the Fe_2As structure with the interstitial Fe replaced by Na atoms.[24] Therefore, NaFeAs consists of a common building block, the FeAs layer, and the double layer of Na^+ sandwiched between the FeAs layers. NaFeAs is expected to be a simplified version of the structure of ReFeAsO (the so-called 1111 system, Re = rare earth) and 122 iron pnictides. There is no static magnetic ordering and structural transition in the isostructural compound LiFeAs,[25,26] which shows superconductivity at 18 K. However, NaFeAs itself has a SDW magnetism with a small magnetic moment (0.09 μ_B/Fe),[13,14,27,28] in contrast to the larger values of magnetic moment ~0.4 μ_B/Fe in the La-"1111"[3] and ~0.9 μ_B/Fe in the Ba-"122" parent compounds.[29] Though NaFeAs shows superconductivity without purposely doping,[24] it possesses only 10% superconducting volume fraction and a long-range AFM order exists in most of its volume inferred from the μSR study on the polycrystalline sample.[13,14] An ARPES experiment on NaFeAs single crystal did not present any signal of a superconducting gap.[30] By doping with Co on a Fe site, bulk superconductivity in NaFeAs can be achieved.[14] A systematic study on the doped NaFeAs single crystals by varying Co concentration has not been done yet. In this paper, we report on the study on the phase diagram of single crystalline $NaFe_{1-x}Co_xAs$ by measuring resistivity, magnetic susceptibility, and specific heat. Additionally, susceptibility shows a temperature-linear dependence up to 500 K for all the superconducting samples, and the deviation from the high-temperature linear behavior occurs in low temperatures, and the deviation temperature increases slightly with increasing the Co concentration. However, such behavior is suddenly changed for the nonsuperconducting overdoped crystal. Analysis on the specific heat of the optimally doped sample revealed a two-band s-wave order symmetry with the sizes of the two gaps at $T = 0$ to be $\Delta_1(0)/k_BT_c = 1.78$ and $\Delta_2(0)/k_BT_c = 3.11$, suggesting strong-coupling superconductivity.

II. EXPERIMENTAL DETAILS

High-quality single crystals of $NaFe_{1-x}Co_xAs$ have been grown by use of the NaAs flux method. NaAs was obtained by reacting the mixture of the elemental Na and As in an evacuated quartz tube at 200 °C for 10 h. Then NaAs, Fe, and Co powders were carefully weighed according to the ratio of NaAs:Fe:Co = 4:1-x:x with (x = 0–0.3), and thoroughly ground. The mixtures were put into alumina crucibles and then sealed in iron crucibles under 1.5 atm of highly pure

 ©2012 American Physical Society

argon gas. The sealed crucibles were heated to 950 °C at a rate of 60 °C/h in the tube furnace filled with the inert atmosphere and kept at 950 °C for 10 h and then cooled slowly to 600 °C at 3 °C/h to grow single crystals. The shiny crystals with typical size of $5 \times 5 \times 0.2$ mm^3 can be easily cleaved from the melt. X-ray diffraction (XRD) was performed on a Smartlab-9 diffracmeter (Rikagu) from 10° to 60° with a scanning rate of 2° per minute. The actual chemical composition of the single crystals is determined by energy dispersive x-ray spectroscopy (EDS). With changing the nominal x from 0 to 0.3, we obtained 13 batches of crystals, whose actual compositions were determined by EDS to be 0, 0.006, 0.010, 0.014, 0.017, 0.021, 0.028, 0.042, 0.047, 0.061, 0.070, 0.075, and 0.109, with the standard instrument error as about 10%. Measurements of resistivity and specific heat were carried out by using the PPMS-9T (Quantum Design). Magnetic susceptibility was measured by using SQUID-MPMS-7T (Quantum Design), and a high-temperature oven was used in the SQUID-MPMS for the magnetic susceptibility measurements above 400 K. In all the magnetic measurements, magnetic field was applied within the *ab* plane.

III. RESULTS AND DISCUSSION

Figure 1(a) shows the selected single-crystalline XRD patterns for the $NaFe_{1-x}Co_xAs$ single crystals. Only (00l) reflections can be recognized, and the rocking curve plotted in the inset of Fig. 1(a) shows a full width at half maximum (FWHM) of about 0.05°, indicating the excellent c-axis orientation and high quality for these single crystals. Lattice parameter of c axis (c) estimated from Fig. 1(a) was plotted as a function of Co concentration, as shown in Fig. 1(b). The lattice parameter, c, of the undoped compound is 7.056 Å, consistent with previous reported results.[14,24] The lattice parameter decreases linearly with increasing Co doping level, consistent with the results reported on the polycrystalline $NaFe_{1-x}Co_xAs$ samples.[14] The amplitude of the change of c (∼1% from 0 to 0.109) is a little larger than that reported in the polycrystalline samples (∼0.4% for the same x region),[14] which lies within a reasonable uncertainty due to the different fabrication methods and crystallizing status.

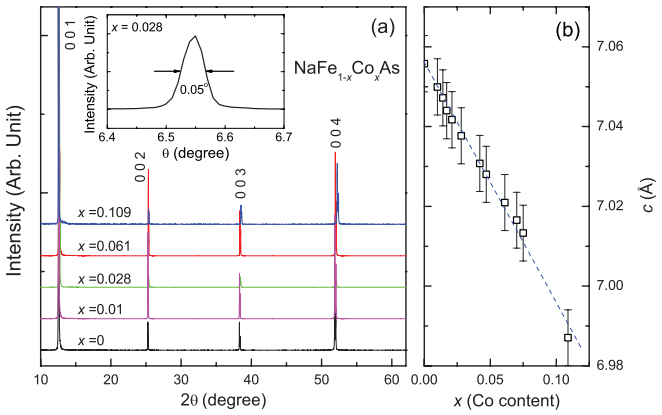

FIG. 1. (Color online) (a) Selected XRD patterns for the $NaFe_{1-x}Co_xAs$ single crystals. (b) The lattice parameter of c axis plotted as a function of the Co concentration x. Inset in (a) is the rocking curve for the (0 0 1) reflection of the crystal with $x = 0.028$.

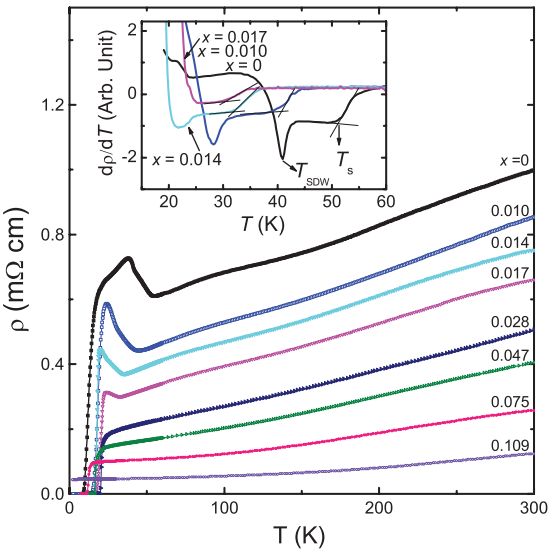

FIG. 2. (Color online) Resistivity as a function of temperature for the $NaFe_{1-x}Co_xAs$ single crystals. Inset is the derivative resistivity for the underdoped $NaFe_{1-x}Co_xAs$ single crystals, where the scenarios to determine the T_s and T_{SDW} are given.

Temperature dependence of resistivity taken from 2 to 300 K were displayed in Fig. 2 for the selected single-crystalline $NaFe_{1-x}Co_xAs$ samples. The resistivity at room temperature decreases with increasing Co doping level. An upturn in resistivity is observed in low temperatures for the underdoped crystals, which arises from the structural/SDW transition. The inset of Fig. 2 shows the derivative of resistivity to figure out the temperatures corresponding to the structural and SDW transitions (T_s and T_{SDW}). The two distinct features in $d\rho(T)/dT$ are used to determine the T_s and T_{SDW}. The structural and SDW transitions are suppressed rapidly with increasing Co concentration. In the samples with Co concentration higher than 2.1%, no trace of structural/SDW transition can be recognized in resistivity. The undoped compound is already superconducting, although the superconducting transition is quite broad, and the resistivity of NaFeAs reaches zero at around 10 K, consistent with previous reports.[24] The superconducting transitions for most of the samples are quite round, so we define the temperature at which resistivity reaches zero as T_c. The optimal doping level is around $x = 0.028$ and the corresponding T_c is 20 K. Further Co doping leads to the decrease of T_c, and no superconducting transition can be observed down to 2 K for the crystal with $x = 0.109$.

Figure 3 shows the magnetic susceptibility taken at 10 Oe in the zero field cooling (ZFC) procedure for the superconducting $NaFe_{1-x}Co_xAs$ single crystals. For $x = 0$, a tiny diamagnetic signal was observed below 9 K, indicating the superconductive shielding effect is weak in this composition of crystal. With enhancing Co doping level, T_c inferred from the diamagnetic signal increases. T_c determined by the susceptibility is nearly the same as that obtained from the resistivity measurements for the crystals with the same composition. The superconductive shielding fraction rises steeply with increasing Co doping level. Full shielding at 2 K can be observed for the crystal by substituting for Fe with 1% Co. The highest T_c of 20 K is obtained in the crystal with $x = 0.028$, and the supercon-

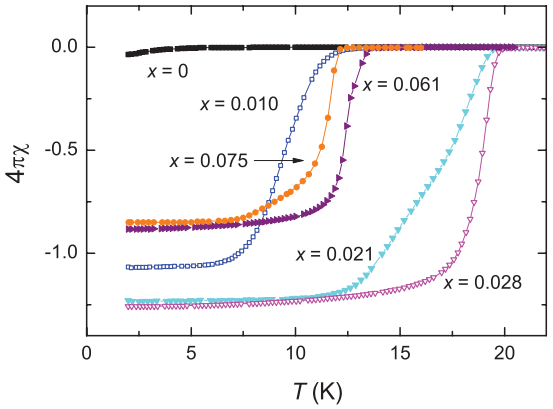

FIG. 3. (Color online) Magnetic susceptibility taken at 10 Oe in ZFC mode for the superconducting samples.

ducting transition is very steep. To our knowledge, this is the best for all the reported crystals in this system. Both shielding fraction and T_c decrease with the further doping of Co.

Susceptibility up to 500 K taken under the magnetic field of 5 T is shown in Fig. 4(a). Because of the very close absolute values of the normal-state susceptibilities for the superconducting samples, the susceptibilities are normalized to the values at 300 K and a shift is then made for all the Co doped samples to distinguish them from each other, as shown in Fig. 4(b). The shift is made by an offset of 0.08 at 300 K from sample to sample by increasing Co concentration. Rapid

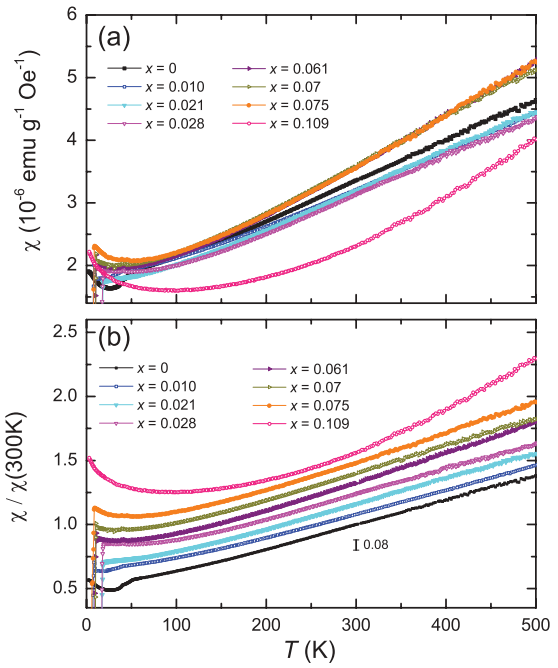

FIG. 4. (Color online) (a) Normal-state susceptibility measured at 5 T in the temperature range up to 500 K for the $NaFe_{1-x}Co_xAs$ single crystals. (b) Normalized normal-state susceptibility for the $NaFe_{1-x}Co_xAs$ single crystals. The susceptibility was normalized to the value at 300 K and shift from sample to sample to distinguish them from each other. The offset at 300 K (=0.08) for the shift of the normalized susceptibility between neighboring sample is also shown in (b).

drops due to superconducting transition can still be observed at low temperature for the doped superconducting samples. For the undoped and underdoped samples, slight kinks can be observed in magnetic susceptibility just above T_c between 20 K and 55 K, which arises from the structural and SDW transitions. Temperature linear dependence can be observed in high temperatures for the magnetic susceptibility of all the superconducting samples. Magnetic susceptibility deviates from the high-temperature linear behavior in low temperatures, and the deviation temperature lies at about 200 K for all the superconducting crystals. With further increasing Co doping level, however, only very weak linear behavior can be found above 400 K in heavily overdoped and nonsuperconducting crystal with $x = 0.109$. The slope for the linear dependence of high-temperature susceptibility is the nearly the same for all the superconducting crystals. Such T-linear dependence of susceptibility has been observed in a lot of parent and doped superconducting iron-pnictides, such as in $Ca_{1-x}Na_xFe_2As_2$,[31] $LaO_{1-x}F_xFeAs$,[32] $Ba(Fe_{1-x}Co_x)_2As_2$,[6,33] and $SrFe_2As_2$.[34] This T-linear behavior resembles that observed in a metallic SDW system above T_{SDW}, such as pure Cr.[35] Such T-linear dependence of magnetic susceptibility is a universal feature for all the iron-based superconductors, which has been theoretically ascribed to the spin fluctuations arising from the local SDW correlation.[36] Antiferromagnetic fluctuations were also considered to enhance the nonanalytic (linear) term in the temperature dependence of susceptibility in a two-dimensional Fermi liquid,[37] which was argued to possibly produce a contribution comparable with such T-linear behavior of susceptibility. Another theoretical interpretation for the T-linear dependence of the susceptibility, which does not need to invoke the antiferromagnetic fluctuations, is taking into account the peculiarities of orbitally resolved densities of states due to local correlations.[38] Whether the T-linear dependent susceptibility in high temperatures is correlated with the pairing force in the high-T_c superconductivity of the iron-based superconducting compounds is still an open question. In the present system, breakdown of the linear dependent susceptibility in the overdoped region coinciding with disappearance of superconductivity seems to suggest the association between T-linear dependence of the susceptibility and superconductivity.

Based on the T_s, T_{SDW}, and T_c inferred from the resistivity and magnetic susceptibility of single crystals, the phase diagram of the $NaFe_{1-x}Co_xAs$ system is established, as shown in Fig. 5. The gradual destruction of magnetism and enhancement of superconductivity (rise of T_c and superconductive shielding fraction) were observed with increasing Co doping level. A dome-shaped T_c vs. x relationship can be observed. Optimal T_c is obtained around $x = 0.028$ and further Co doping suppresses superconductivity. T_c goes to zero around $x = 0.109$. This phase diagram is very close to that sketched from polycrystalline samples.[14] This phase diagram is also quite similar to those of 122 and 1111 systems except that the starting compound of the present system is superconducting. In addition, the optimal T_c can be achieved by about 2.8% Co doping in $NaFe_{1-x}Co_xAs$, much less than ~7% Co in the $Ba(Fe_{1-x}Co_x)_2As_2$ system.[39,40] From this point of view, the phase diagram of $NaFe_{1-x}Co_xAs$ is more similar to that of the $Ba(Fe_{1-x}Ni_x)_2As_2$ system,[41] in which the optimal doping

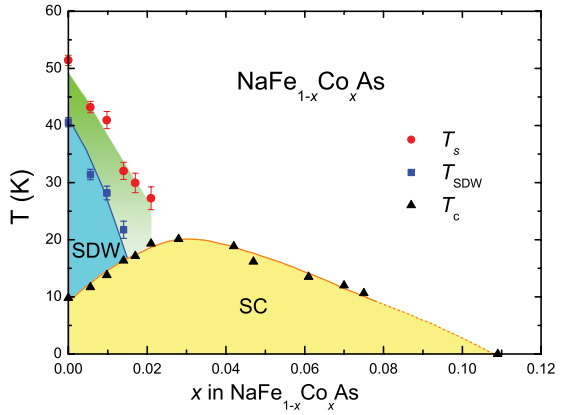

FIG. 5. (Color online) Phase diagram of $NaFe_{1-x}Co_xAs$. T_s, T_{SDW}, and T_c are determined from the resistivity in Fig. 2 and its inset. Susceptibility in Fig. 3 and Fig. 4 give almost the same value for T_s, T_{SDW}, and T_c. The solid lines guide the eye. The dashed line used to display the evolution of T_c between $0.075 < x < 0.109$ is plotted to indicate the uncertainty of the end point for $T_c = 0$.

is reached at the 4.6% doping, far from that at the ~7% doping in $Ba(Fe_{1-x}Co_x)_2As_2$.

Figures 6(a) and 6(b) display the temperature dependence of the low-temperature specific heat (plotted as C_p/T) for the underdoped to heavily overdoped crystals. The specific heat for the undoped samples shown in Fig. 6(a) exhibit two anomalies corresponding to the structural and SDW transitions, respectively. The inferred T_s and T_{SDW} are very consistent with those determined from resistivity in the inset of Fig. 2. No anomaly corresponding to the superconducting transition can be observed in the specific heat for the undoped sample, which could be due to the low fraction of the superconducting component. This is consistent with the tiny superconducting shielding fraction from the susceptibility measurement shown in Fig. 3. For the crystal with $x = 0.014$, a clear anomaly corresponding to the superconducting transition can be observed around 14 K, indicating bulk superconductivity in this sample and consistent with the good superconductive shielding for the crystals with $x > 0.01$ (as shown Fig. 3). In addition, an anomaly is observed at about 33 K, which coincides with the structural transition determined by the derivative of resistivity shown in the inset of Fig. 2. However, only a very obscure anomaly corresponding to SDW transition is observed around 22 K. In order to watch the structural, SDW, and superconducting transitions clearly, the derivative of the specific heat for the crystal with $x = 0.014$ is shown in Fig. 6(b), and it clearly shows three dips at T_s, T_{SDW}, and T_c, indicating the coexistence of the antiferromagnetism and superconductivity for this underdoped crystal. The specific heat of the heavily overdoped and nonsuperconducting crystal with $x = 0.109$ does not show any anomaly. As temperature increases, the specific heat above T_s for the sample with $x = 0.014$ tends to be the same as that of the sample with $x = 0.109$.

A pronounced jump due to the superconducting transition can be observed in the temperature dependence of specific heat for the optimally doped and overdoped superconducting samples, as shown in Fig. 6(c). The normal-state specific heat, C_p, can be described by $C_p = C_{en} + C_{lattice}(T)$ with

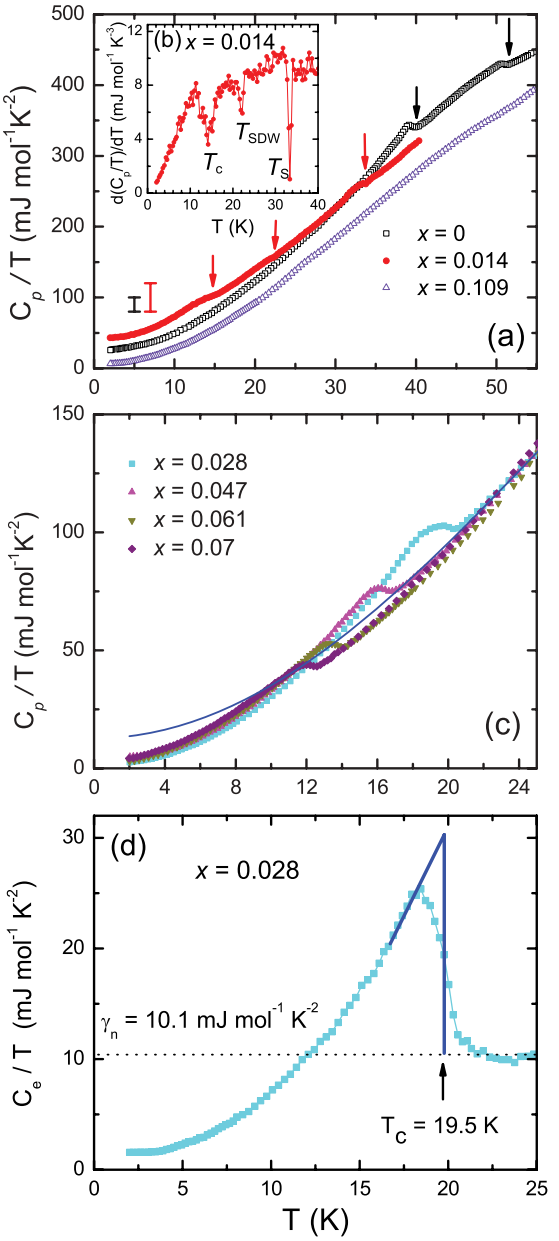

FIG. 6. (Color online) (a) Temperature dependence of the low-temperature specific heat (C_p/T) for the underdoped and heavily overdoped $NaFe_{1-x}Co_xAs$ crystals. The arrows points to the anomalies in the specific heat. To give a good vision effect, C_p/T of the undoped and underdoped crystals has been shifted upward from that of the heavily overdoped sample, with the offsets of 20 and 40 mJ/mol K^2, respectively (as shown in the panel). (b) The inset shows the derivative of the specific heat for the crystal with $x = 0.014$, where the structural, SDW, and superconducting transitions can be clearly recognized from the dips. (c) Specific heat as a function of temperature for the optimally doped and overdoped superconducting $NaFe_{1-x}Co_xAs$ crystals. The blue line is the fitting of the specific heat between 20 and 40 K by using $C_p = C_{en} + C_{lattice}$. (d) Electronic specific heat C_e/T (by subtracting the lattice contribution from C_p/T) as a function of temperature for the optimally doped crystal, where the dashed line represents the normal-state electronic contribution, $\gamma_n = 10.1$ mJ mol^{-1} K^{-2}.

the electronic contribution of $C_{en} = \gamma_n T$ and the lattice contribution of $C_{lattice}(T) = \beta T^3 + \delta T^5$. The solid line in

Fig. 6(c) is the best fit to the C_p/T above T_c (20 K to 40 K) for the optimally doped sample, yielding $\gamma_n = 10.1$ mJ/mol K^{-2}, $\beta = 0.23$ mJ/mol K^{-4}, and $\delta = -0.0589$ μJ/mol K^{-6}. After subtracting this C_{lattice} component, the obtained results are shown in Fig. 6(d), for which the entropy conservation is confirmed to be satisfied. Figure 6(d) indicates that C_e/T does not extrapolate to zero at the $T = 0$ limit but to a finite residual normal-state-like contribution, $\gamma_r = 1.5$ mJ mol^{-1} K^{-2}. Finite values of γ_r are a common feature in the specific measurements of the iron-based superconductors.[42,43]

The normalized electron specific heat is displayed in Fig. 7. Considering the existence of γ_r, the electronic specific heat for one mole of superconducting material can be defined as $C_{\text{es}} = (C_e - \gamma_r T)\frac{\gamma_n}{\gamma_n - \gamma_r}$, which has been used in Ref. 42 for $Ba(Fe_{1-x}Co_x)_2As_2$[42] and in Ref. 43 for $Ba_{0.65}Na_{0.35}Fe_2As_2$.[43] As interpreted in Ref. 42, C_{es} can be expected to be a reasonable and useful approximation to the specific heat of a mole of superconducting material. C_{es} was then used in Fig. 7. Figure 7(a) indicates that C_{es} cannot be described by a single band BCS superconductor, calculated either in the weak-coupling limit with $\alpha = \Delta(0)/k_B T_c = 1.764$ or by letting α be adjustable. Notably, the fitting in the weak-coupling limit shows very poor agreement with the experimental data. Figure 7(a) also shows the fitting results by using the BCS single-band d-wave model.[45] It is clear that such a k-dependent gap, even in the strong coupling scenario (obtained $\alpha = 3.45$), cannot describe the observed data. As a result, the phenomenological two-band α model with two energy gaps was used, and the fitting results are shown in Fig. 7(b). The two-band α model results in an excellent fitting of the specific heat from $T_c/10$ to T_c, and, as a consequence, gives the reliable gaps. This fitting is calculated as the sum of the contributions from two bands by assuming independent BCS temperature dependencies of the two superconducting gaps, as shown by the dashed and short-dashed lines in Fig. 7(b). In the fitting, the magnitudes of two gaps at the $T = 0$ limit are introduced as adjustable parameters, $\alpha_1 = \Delta_1(0)/k_B T_c$ and $\alpha_2 = \Delta_2(0)/k_B T_c$. At the same time, γ_i/γ_n ($i = 1, 2$), which measures the fraction of the total normal electron density of states, are introduced as adjustable parameters. The obtained α_1 for the small gap is 1.78, and α_2 for the large gap is 3.11. The relative weight for the small and large gaps here is $\gamma_2/\gamma_1 = 0.72$. Both of the obtained two gaps are larger than that of the BCS weak-coupling limit. This is not consistent with the theoretical constraints that one gap must be larger than the BCS gap and one smaller in a weakly coupled two-band superconductor,[44] which has been observed in MgB_2[46] and another iron-based superconductor $Ba(Fe_{0.925}Co_{0.075})_2As_2$[42] and $Ba_{0.65}Na_{0.35}Fe_2As_2$[43] as well as another 111 superconductor, LiFeAs.[19] Actually, such a phenomenon, where the two gaps are larger than the BCS weak-coupling limit, has been also observed in the $Fe(Te_{0.57}Se_{0.43})$[47] and $Ba_{0.6}K_{0.4}Fe_2As_2$[48] single crystals. The large magnitudes of the gaps derived from our fitting suggest the strong-coupling superconductivity, as that reported in $Fe(Te_{0.57}Se_{0.43})$ previously.[47] The relative ratio of the two gaps in $NaFe_{0.972}Co_{0.028}As$ is $\Delta_1(0)/\Delta_2(0) \sim 0.57$, which is a little larger than that seen in other iron-pnictide superconductors where $\Delta_1(0)/\Delta_2(0) = 0.3 \sim 0.5$.[42,43,49–51]

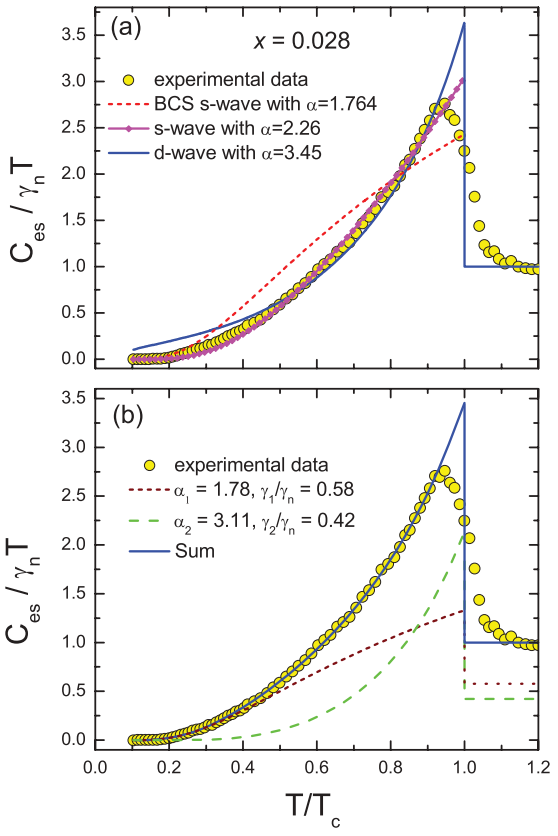

FIG. 7. (Color online) (a) The normalized electron specific heat of the optimally doped crystal with $x = 0.028$, compared with the specific heat of single-band s-wave (magenta dotted line) and d-wave (blue solid line) order parameters as well as that in the weak-coupling limit (red dashed line). (b) The normalized electron specific heat of the superconducting sample with $x = 0.028$. The blue solid curve represents a two-gap s-wave fit. The brown short-dashed and green long-dashed curves are the partial specific-heat contributions of the two bands.

It should be noted that the employed α model here follows a simple semiempirical approach in which the superconducting gap is assumed to have BCS temperature dependence and the interband coupling is not taken into account. A γ model was proposed by Kogan *et al.*[52] as an effective approach to take into account the interband coupling. One should note that, although in the present work the fitting of specific heat suggests isotropic gaps, some theoretical and other experiments also suggest complicated pair symmetry for most of iron-based superconductors, including the nodeless anisotropic or nodal gaps. Therefore, further detailed theoretical analysis on our experimental data with such a γ model and other appropriate models, involving proper gap symmetry, may be required to achieve full understanding of the multigap nature in the iron-based superconductors. Actually, some detailed information on the superconducting gap structure in $NaFe_{1-x}Co_xAs$ system has been achieved from other approaches very recently. Among them, the penetration depth experiment indicates a nodal gap in the optimally doped crystal,[15] however, ARPES, STM, and heat transport measurements revealed nodeless gaps in the optimally doped and overdoped crystals.[16,17,23] Our results supports the nodeless gap symmetry observed by the ARPES experiment.[16] Notably, our analysis is consistent with

the existence of different magnitudes of the gaps suggested by STM and heat transport.[17,23]

IV. CONCLUSION

In summary, we mapped out the phase diagram of the $NaFe_{1-x}Co_xAs$ system through measuring the transport and magnetic properties on high-quality single crystals. Substitution of Co for Fe destroys both the structural and magnetic transitions; however, it enhances the T_c and the superconducting shielding fraction. Susceptibility exhibits a T-linear dependence in the high temperatures up to 500 K for all the superconducting samples; however, such behavior cannot be observed in the nonsuperconducting overdoped crystal. The breakdown of the linear dependent susceptibility in the overdoped region coinciding with disappearance of superconductivity seems to suggest the association between the T-linear dependence of the susceptibility and superconductivity. Analysis on the specific heat in the superconducting state reveals a two-band s-wave order parameter with gap amplitudes of $\Delta_1(0)/k_BT_c = 1.78$ and $\Delta_2(0)/k_BT_c = 3.11$, suggesting strong-coupling superconductivity.

ACKNOWLEDGMENTS

This work is supported by the National Natural Science Foundation of China (Grants No. 11190021 and No. 51021091), the National Basic Research Program of China (973 Program, Grants No. 2012CB922002 and No. 2011CB00101), and the Chinese Academy of Sciences.

*Corresponding author: chenxh@ustc.edu.cn

[1] Y. Kamihara, H. Hiramatsu, M. Hirano, R. Kawamura, H. Yanagi, T. Kamiya, and H. Hosono, J. Am. Chem. Soc. **128**, 10012 (2006).
[2] X. H. Chen, T. Wu, G. Wu, R. H. Liu, H. Chen, and D. F. Fang, Nature (London) **453**, 761 (2008).
[3] C. de la Cruz, Q. Huang, J. W. Lynn, J. Y. Li, W. Ratcliff ll, J. L. Zarestky, H. A. MooK, G. F. Chen, J. L. Luo, N. L. Wang, and P. C. Dai, Nature (London) **453**, 899 (2008).
[4] M. Rotter, M. Tegel, and D. Johrendt, Phys. Rev. Lett. **101**, 107006 (2008).
[5] X. F. Wang, T. Wu, G. Wu, H. Chen, Y. L. Xie, J. J. Ying, Y. J. Yan, R. H. Liu, and X. H. Chen, Phys. Rev. Lett. **102**, 117005 (2009).
[6] X. F. Wang, T. Wu, G. Wu, R. H. Liu, H. Chen, Y. L. Xie, and X. H. Chen, New J. Phys. **11**, 045003 (2009).
[7] C. Lester, J. H. Chu, J. G. Analytis, S. C. Capelli, A. S. Erickson, C. L. Condron, M. F. Toney, I. R. Fisher, and S. M. Hayden, Phys. Rev. B **79**, 144523 (2009).
[8] R. W. Hu, S. L. Bud'ko, W. E. Straszheim, and P. C. Canfield, Phys. Rev. B **83**, 094520 (2011).
[9] M. Zhang, J. J. Ying, Y. J. Yan, A. F. Wang, X. F. Wang, Z. J. Xiang, G. J. Ye, P. Cheng, X. G. Luo, J. P. Hu, and X. H. Chen, Phys. Rev. B **85**, 092503 (2012).
[10] T. Goko *et al.*, Phys. Rev. B **80**, 024508 (2009).
[11] F. L. Ning, K. Ahilan, T. Imai, A. S. Sefat, R. Y. Jin, M. A. McGuire, B. C. Sales, and D. Mandrus, J. Phys. Soc. Jpn. **78**, 013711 (2009).
[12] H. Chen, Y. Ren, Y. Qiu, Wei Bao, R. H. Liu, G. Wu, T. Wu, Y. L. Xie, X. F. Wang, Q. Huang, and X. H. Chen, Europhys. Lett. **85**, 17006 (2009).
[13] J. D. Wright, T. Lancaster, I. Franke, A. J. Steele, J. S. Möller, M. J. Pitcher, A. J. Corkett, D. R. Parker, D. G. Free, F. L. Pratt, P. J. Baker, S. J. Clarke, and S. J. Blundell, Phys. Rev. B **85**, 054503 (2012).
[14] D. R. Parker, M. J. P. Smith, T. Lancaster, A. J. Steele, I. Franke, P. J. Baker, F. L. Pratt, M. J. Pitcher, S. J. Blundell, and S. J. Clarke, Phys. Rev. Lett. **104**, 057007 (2010).
[15] K. Cho, M. A. Tanatar, N. Spyrison, H. Kim, G. Tan, P. Dai, C. L. Zhang, and R. Prozorov, arXiv:1201.2966.
[16] Z.-H. Liu, P. Richard, K. Nakayama, G.-F. Chen, S. Dong, J.-B. He, D.-M. Wang, T.-L. Xia, K. Umezawa, T. Kawahara, S. Souma, T. Sato, T. Takahashi, T. Qian, Yaobo Huang, Nan Xu, Yingbo Shi, H. Ding, and S.-C. Wang, Phys. Rev. B **84**, 064519 (2011).
[17] S. Y. Zhou, X. C. Hong, X. Qiu, B. Y. Pan, Z. Zhang, X. L. Li, W. N. Dong, A. F. Wang, X. G. Luo, X. H. Chen, and S. Y. Li, arXiv:1204.3440.
[18] F. Wei, F. Chen, K. Sasmal, B. Lv, Z. J. Tang, Y. Y. Xue, A. M. Guloy, and C. W. Chu, Phys. Rev. B **81**, 134527 (2010).
[19] D. J. Jang, J. B. Hong, Y. S. Kwon, T. Park, K. Gofryk, F. Ronning, J. D. Thompson, and Y. Bang, arXiv:1203.1362.
[20] U. Stockert, M. Abdel-Hafiez, D. V. Evtushinsky, V. B. Zabolotnyy, A. U. B. Wolter, S. Wurmehl, I. Morozov, R. Klingeler, S. V. Borisenko, B. Büchner, arXiv:1011.4246.
[21] M. A. Tanatar, J.-P. Reid, S. René de Cotret, N. Doiron-Leyraud, F. Laliberte, E. Hassinger, J. Chang, H. Kim, K. Cho, Y. J. Song, Y. S. Kwon, R. Prozorov, and L. Taillefer, Phys. Rev. B **84**, 054507 (2011).
[22] D. S. Inosov, J. S. White, D. V. Evtushinsky, I. V. Morozov, A. Cameron, U. Stockert, V. B. Zabolotnyy, T. K. Kim, A. A. Kordyuk, S. V. Borisenko, E. M. Forgan, R. Klingeler, J. T. Park, S. Wurmehl, A. N. Vasiliev, G. Behr, C. D. Dewhurst, and V. Hinkov, Phys. Rev. Lett. **104**, 187001 (2010); S. V. Borisenko, V. B. Zabolotnyy, D. V. Evtushinsky, T. K. Kim, I. V. Morozov, A. N. Yaresko, A. A. Kordyuk, G. Behr, A. Vasiliev, R. Follath, and B. Buchner, *ibid.* **105**, 067002 (2010).
[23] H. Yang, Z. Y. Wang, D. L. Fang, T. Kariyado, G. F. Chen, M. Ogata, T. Das and A. V. Balatsky and H. H. Wen, arXiv:1203.3123.
[24] D. R. Parker, M. J. Pitcher, P. J. Baker, I. Franke, T. Lancaster, S. J. Blundell, and S. J. Clarke, Chem. Commun. **2009**, 2189 (2009).
[25] X. C. Wang, Q. Q. Liu, Y. X. Lv, W. B. Gao, L. X. Yang, R. C. Yu, F. Y. Li, and C. Q. Jin, Solid State Commun. **148**, 538 (2008).
[26] N. Qureshi, P. Steffens, Y. Drees, A. C. Komarek, D. Lamago, Y. Sidis, L. Harnagea, H.-J. Grafe, S. Wurmehl, B. Buchner, and M. Braden, Phys. Rev. Lett. **108**, 117001 (2012).
[27] S. Li, C. de la Cruz, Q. Huang, G. F. Chen, T.-L. Xia, J. L. Luo, N. L. Wang, and P. Dai, Phys. Rev. B **80**, 020504(R) (2009).
[28] L. Ma, G. F. Chen, D. X. Yao, J. Zhang, S. Zhang, T.-L. Xia, and W. Q. Yu, Phys. Rev. B **83**, 132501 (2011).
[29] Q. Huang, Y. Qiu, W. Bao, M. A. Green, J. W. Lynn, Y. C. Gasparovic, T. Wu, G. Wu, and X. H. Chen, Phys. Rev. Lett. **101**, 257003 (2008).

[30]C. He, Y. Zhang, B. P. Xie, X. F. Wang, L. X. Yang, B. Zhou, F. Chen, M. Arita, K. Shimada, H. Namatame, M. Taniguchi, X. H. Chen, J. P. Hu, and D. L. Feng, Phys. Rev. Lett. **105**, 117002 (2010).

[31]G. Wu, H. Chen, T. Wu, Y. L. Xie, Y. J. Yan, R. H. Liu, X. F. Wang, J. J. Ying, and X. H. Chen, J. Phys.: Condens. Matt. **20**, 422201 (2008).

[32]R. Klingeler, N. Leps, I. Hellmann, A. Popa, U. Stockert, C. Hess, V. Kataev, H.-J. Grafe, F. Hammerath, G. Lang, S. Wurmehl, G. Behr, L. Harnagea, S. Singh, and B. Büchner, Phys. Rev. B **81**, 024506 (2010).

[33]X. F. Wang, T. Wu, G. Wu, H. Chen, Y. L. Xie, J. J. Ying, Y. J. Yan, R. H. Liu, and X. H. Chen, Phys. Rev. Lett. **102**, 117005 (2009).

[34]J.-Q. Yan, A. Kreyssig, S. Nandi, N. Ni, S. L. Bud'ko, A. Kracher, R. J. McQueeney, R. W. McCallum, T. A. Lograsso, A. I. Goldman, and P. C. Canfield, Phys. Rev. B **78**, 024516 (2008).

[35]E. Fawcett, H. L. Alberts, V. Yu. Galkin, D. R. Noakes, and J. V. Yakhmi, Rev. Mod. Phys. **66**, 25 (1994).

[36]G. M. Zhang, Y. H. Su, Z. Y. Lu, Z. Y. Weng, D. H. Lee, and T. Xiang, Europhys. Lett. **86**, 37006 (2009).

[37]M. M. Korshunov, I. Eremin, D. V. Efremov, D. L. Maslov, and A. V. Chubukov, Phys. Rev. Lett. **102**, 236403 (2009).

[38]S. L. Skornyakov, A. A. Katanin, and V. I. Anisimov, Phys. Rev. Lett. **106**, 047007 (2011).

[39]N. Ni, M. E. Tillman, J.-Q. Yan, A. Kracher, S. T. Hannahs, S. L. Bud'ko, and P. C. Canfield, Phys. Rev. B **78**, 214515 (2008).

[40]J. H. Chu, J. G. Analytis, C. Kucharczyk, and I. R. Fisher, Phys. Rev. B **79**, 014506 (2009).

[41]N. Ni, A. Thaler, J. Q. Yan, A. Kracher, E. Colombier, S. L. Bud'ko, P. C. Canfield, and S. T. Hannahs, Phys. Rev. B **82**, 024519 (2010).

[42]F. Hardy, T. Wolf, R. A. Fisher, R. Eder, P. Schweiss, P. Adelmann, H. v. Löhneysen, and C. Meingast, Phys. Rev. B **81**, 060501(R) (2010).

[43]A. K. Pramanik, M. Abdel-Hafiez, S. Aswartham, A. U. B. Wolter, S. Wurmehl, V. Kataev, and B. Büchner, Phys. Rev. B **84**, 064525 (2011).

[44]C. L. Huang, J.-Y. Lin, C. P. Sun, T. K. Lee, J. D. Kim, E. M. Choi, S. I. Lee, and H. D. Yang, Phys. Rev. B **73**, 012502 (2006).

[45]V. Z. Kresin and S. A. Wolf, Physica C **169**, 476 (1990).

[46]F. Bouquet, Y. Wang, R. A. Fisher, D. G. Hinks, J. D. Jorgensen, A. Junod, and N. E. Philips, Europhys. Lett. **56**, 567 (2001).

[47]J. Hu, T. J. Liu, B. Qian, A. Rotaru, L. Spinu, and Z. Q. Mao, Phys. Rev. B **83**, 134521 (2011).

[48]F. Y. Wei, B. Lv, Y. Y. Xue, and C. W. Chu, Phys. Rev. B **84**, 064508 (2011).

[49]K. Gofryk, A. S. Sefat, E. D. Bauer, M. A. McGuire, B. C. Sales, D. Mandrus, J. D. Thompson, and F. Ronning, New J. Phys. **12**, 023006 (2010).

[50]F. Hardy, P. Burger, T. Wolf, R. A. Fisher, P. Schweiss, P. Adelmann, R. Heid, R. Fromknecht, R. Eder, D. Ernst, H. v. Loehneysen, and C. Meingas, Europhys. Lett. **91**, 47008 (2010).

[51]P. Popovich, A. V. Boris, O. V. Dolgov, A. A. Golubov, D. L. Sun, C. T. Lin, R. K. Kremer, and B. Keimer, Phys. Rev. Lett. **105**, 027003 (2010).

[52]V. G. Kogan, C. Martin, and R. Prozorov, Phys. Rev. B **80**, 014507 (2009).